

FULL PAPER

A Tripodal Ruthenium(II) Polypyridyl Complex with pH Controlled Emissive Quenching

Rodney T. Brown,^[b] Nicholas C. Fletcher,^{*[a,b]} Lefteris Danos^[a] and Nathan R. Halcovitch^[a]

Abstract: A tripodal podand has been prepared and complexed to ruthenium(II) creating a metal complex with C_3 -symmetry and an enclosed cavity. The complex shows the anticipated enhanced emission when compared to $[\text{Ru}(\text{bipy})_3]^{2+}$ in acetonitrile. The emission from this cryptand like structure is invariant to the introduction of monovalent cations in aqueous solution, but a significant drop in the emission was observed with increasing pH over a very broad pH range (3 to 12). This is attributed to an N to t_{2g} electron transfer in the excited-state in the unprotonated form with a transfer rate of the order of $4.2 \times 10^5 \text{ s}^{-1}$. The crystal structure indicates the inclusion of water within the cavity suggesting that the protonation of a tertiary amine can be effectively moderated by a water molecule held in close proximity within a rigid cavity.

Introduction

Hexadentate tethered tris-diimine ligands, commonly described as podands, upon chelation to transition metal ions with labile groups have been shown to readily form complexes.^[1] These have a *fac* orientated geometry and a pseudo-octahedral coordination environment at the metal center provided the connection between the three bidentate functions is of an appropriate length. If the controlling tether is short, it either distorts the structure towards trigonal prismatic geometry,^[1f] or encourages the formation of dimers.^[1o] If the podand ligand is sufficiently large, the coordination of the metal results in an enclosed tripodal space reminiscent of a cryptand like cavity.^[2] Such systems have allowed relocation of a labile metal ion, with for example Lutz *et al.* demonstrating that, iron can switch between three 2,2'-bipyridine and a salicylamide groups by changing the oxidation state.^[1g,1h,1i] This ability to change coordination mode is dependent on the nature of the cavity, and the selection of functional groups.^[3] Alternatively, the inclusion of suitable hydrogen bond donating groups can allow the selective encapsulation of anions.^[1a,1b,1i,4]

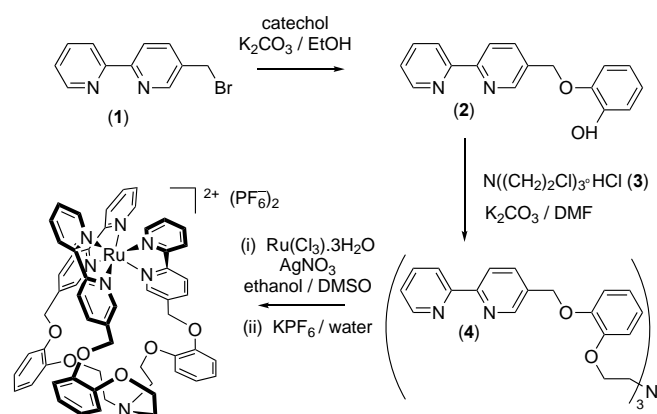
The functionalized polypyridine complexes of ruthenium(II) have attracted considerable attention^[5] with potential applications in solar cells,^[6] water splitting^[7] and the photocatalytic reduction

of carbon dioxide.^[8] They have also been shown to have specific interactions with biological structures^[9] such as DNA^[10] and proteins,^[11] and have recently been shown to be excellent as time-gated cell imaging^[10,12] and antimicrobial agents.^[13] Tris-diimine complexes of ruthenium(II) however can undergo ligand photo-substitution reactions; for $[\text{Ru}(\text{bipy})_3]^{2+}$ in aqueous solution, the quantum yield of photodecomposition (ϕ_p) is in the range 10^{-5} - 10^{-3} , depending on pH and temperature.^[14] In solutions containing X^- ions such as Cl^- , Br^- , and NCS^- the value of ϕ_p may be as high as 10^{-1} in solvents with low dielectric constant.^[15] Linking together the three bidentate ligands to form a cage reduces the chance of decomposition, for example in a system constructed on the metal center showed that photo-dissociation can be reduced by a factor of 10^4 when compared to $[\text{Ru}(\text{bipy})_3]^{2+}$, potentially enhancing the longevity of compounds in photoactive devices.^[16] Additionally, by forming a cage like architecture around the metal ion, the long lived ³MLCT emissive state can be enhanced as it reduces access to thermally distorted structures that can lead to population of the ³MC state and radiationless decay.^[17]

The formation of tris-diimine podand type structures with Ru(II) is however more challenging than with first row transition metal complexes. Due to the stability of the $4d^6$ low spin configuration, the kinetically, rather than the thermodynamically, favored product is typically isolated, and there can also be complications of *mer* versus *fac* coordination geometries.^[18] This often results in a mixture of species, with high order nuclearity, difficult purification procedures and low yields. For example, a tris(bipyridine-imidazolium) ligand reported by Sato, gave a 91% yield with Fe^{2+} , but only 46% with Ru^{2+} , whilst a more recent example Nabeshima and co-workers show similar differences,^[11] and the systems reported by Oylar *et al.*^[19] and Weizman *et al.*^[20] only achieved yields in the region of 25% despite using high reaction temperatures. In our experience, yields are often observed to be disappointingly low, especially with the more rigid of systems,^[21] but high dilution conditions can overcome this to a certain extent, with a yield of 85% being achieved in one exceptional case.^[22] The tether itself can also play a crucial role in the determination of the metal centered stereochemistry. In several examples it has been shown to determine the metal centered helicity,^[19-20,21c,23] and can even be removed to form a true *fac* orientated inert chelate.^[20,21b,21c,22]

Yet the rewards of isolating a species with a long lived fluorescent unit such as $[\text{Ru}(\text{bipy})_3]^{2+}$ adjacent to an enclosed three dimensional cavity offers significant opportunities for the selective recognition of small molecules.^[24] It has been shown to be of interest in the selective detection of anions,^[4b,19,21a] but this has not been replicated with the successful recognition of cations. Nabeshima *et al.* have reported a cavity with a suitable extended cavity space with a degree of selectivity for divalent cations such as Ca^{2+} and Mg^{2+} , but the protonation of a central nitrogen resulted in some interesting and unexplained effects.^[11]

- [a] Dr. N.C. Fletcher, Dr. L. Danos and Dr N.R. Halcovitch
Department of Chemistry
Lancaster University
Bailrigg, Lancaster, LA1 4YB, UK
E-mail: n.fletcher@lancaster.ac.uk
Homepage: www.lancaster.ac.uk/chemistry/people/nick-fletcher
- [b] Dr. R.T. Brown, and Dr. N.C. Fletcher
School of Chemistry and Chemical Engineering,
Queen's University Belfast,
Belfast, Northern Ireland, BT9 5AG, UK



Scheme 1. Synthetic route to the ruthenium(II) tripodal podand.

We too were curious whether we could also prepare a cationic species capable of recognizing a cation within a similarly enclosed cavity. In the subsequent report we highlight an interesting system with detection of a proton exhibiting some surprising optical behavior, and the absence of direct cation binding.

Results and Discussion

The preparation of the proposed tripodal hexadentate ligand was achieved in reasonable yield (Scheme 1). 5-Bromomethyl-2,2'-bipyridine (**1**) was initially prepared from 5-methyl-2,2'-bipyridine using the standard radical initiated reaction with *N*-bromosuccinimide in a disappointing yield of 39%.^[25] As an alternative, it was also isolated via deprotonation of 5-methyl-2,2'-bipyridine using LDA and reaction with trimethylsilylchloride to afford the TMS intermediate in good yield.^[26] Savage *et al.* report that the TMS group can be readily removed *in situ* using CsF, giving **1** by reaction with 1,2-dibromotetrafluoroethane. As an alternative to this, we stirred 5-(trimethylsilyl)-methyl-2,2'-bipyridine with bromine in the presence of CsF in DMF, isolating the precursor in a disappointing 27% yield following column chromatography. The brominated precursor (**1**) was reacted with catechol in ethanol in the presence of a mild base, giving the targeted product in an unoptimized yield of 42%. The resulting oily product was introduced in slight excess to a methanolic solution of tris-2-chloroethylamine hydrochloride (**3**)^[27] (extreme care must be exercised in the synthesis and handling this compound as it is a mustard agent with severe vesicant properties and isolated and used under temporary license), followed by NaH using similar conditions to those employed by Nabeshima *et al.*^[14] resulting in the targeted podand (**4**) in a 79 % yield.

Complexation of **4** with Ru(II) was achieved by the slow addition of $\text{RuCl}_3 \cdot x\text{H}_2\text{O}$ dissolved in a large volume of a refluxing 10% DMSO / ethanol mixture containing a slight excess of AgNO_3 . A range of polynuclear products were removed by cation-exchange chromatography (Sephadex® C-25) eluting the target mononuclear complex with a 0.3 M aqueous NaCl solution and isolated by precipitation as the hexafluorophosphate salt. This was then purified by repeated recrystallization from acetone/water to give a red solid in a yield of 35 %. The identity of the product was confirmed by ESI mass spectrometry with the observation of the molecular ion less one and two hexafluorophosphate ions.

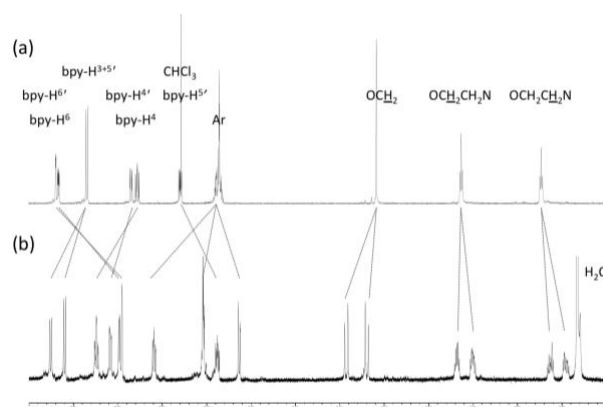


Figure 1. ^1H NMR spectra of a) Compound **4** (in CDCl_3) and b) $[\text{Ru}(\mathbf{4})](\text{PF}_6)_2$ in $(\text{CD}_3)_2\text{O}$ at 298 K.

The ^1H NMR spectrum of complex $[\text{Ru}(\mathbf{4})](\text{PF}_6)_2$ displays a number of interesting features (Figure 1). The methylene protons in the complex are diastereotopic and appear as an AB set presenting as doublets at 5.24 and 5.43 ppm with the typical geminal coupling of 14.5 Hz, which is good evidence of the proposed structure in solution. These are significantly downfield of the corresponding protons in the free ligand, and also downfield of the methylene protons in the previously reported^[21b] *fac*-alcohol complex $[\text{Ru}(\text{bipy-CH}_2\text{OH})_3](\text{PF}_6)_2$ (4.60 ppm), probably due to an increased deshielding effect from the adjacent aromatic ring. There are small but significant differences between these two compounds in the bipyridine proton signals, most notably with the H^3 proton. Additionally, the ethylene CH_2 protons are also diastereotopic suggesting that a rigid structure is adopted by the ligand upon complexation.

Crystals of the hexafluorophosphate salt $[\text{Ru}(\mathbf{4})](\text{PF}_6)_2$ were subsequently isolated by the slow evaporation from acetone / methanol, whilst attempts were made to make the product soluble in aqueous solution by the attempted conversion to the chloride salt using ion-exchange resin. The resulting crystals obtained by slow evaporation of the aqueous / acetonitrile were determined by X-ray crystallography. The resulting metal complex was present, however the anticipated chloride anions were not detected, but the open cavities surrounding the complexes contained a network of water. It is therefore assumed that a hydroxide salt $[\text{Ru}(\mathbf{4})](\text{OH})_2$ had been obtained, although it could potentially be as a result of a disordered fluoride anion and may not be representative of the bulk sample.

A comparison of the two different structures proved interesting. Complex $[\text{Ru}(\mathbf{4})](\text{OH})_2$ crystallizes in the hexagonal space group R-3, with the three ligands around the metal centers being symmetry related reflecting the C_3 -symmetry of the complex (Figure 2). The unit cell contains six units aligned along the long *c*-axis with the Ru-N bond lengths (2.075(4)Å and 2.055(4)Å) and angles of 93.78(15)°, 92.39(15)° and 170.42(15)° similar to published *fac*-configured structures suggesting that the tether does not cause any significant strain to the metal center, and that the complex retains the 2+ oxidation state despite not determining the position of the counter anions.^[22,28] In fact the metal centered coordination geometry, RuN_6 , is close to being an ideal octahedral, and similar to many related species in the CCDC database. One interesting feature is the close intermolecular separation between the aromatic catechol and the bipyridine rings,

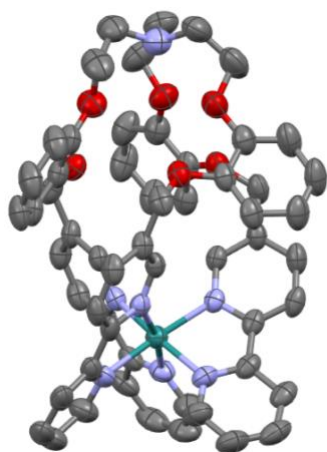


Figure 2. The structure of $[\text{Ru}(\mathbf{4})](\text{OH})_2$ units with ellipsoids at 50% probability. Hydrogen atoms, solvent and the anions have been deleted for clarity.

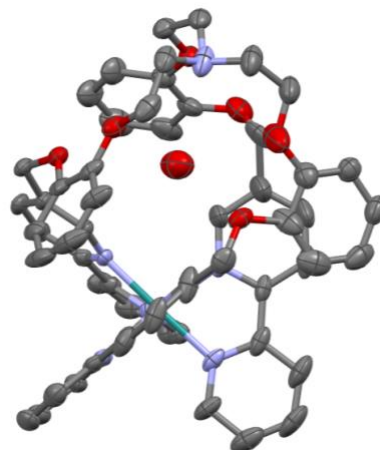


Figure 4. The structure of $[\text{Ru}(\mathbf{4})](\text{PF}_6)_2$ units with ellipsoids at 50% probability. Hydrogen atoms, solvent and the anions have been deleted for clarity.

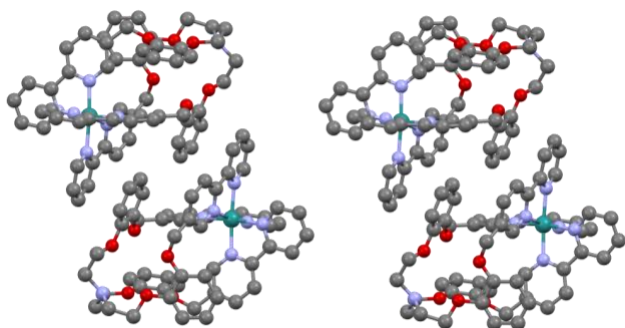


Figure 3 Illustration of the inter- and intramolecular π -stacking interactions within the structure of $[\text{Ru}(\mathbf{4})](\text{OH})_2$.

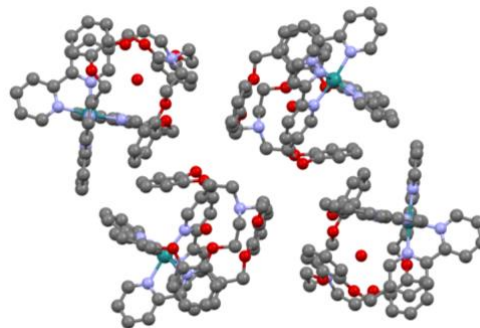


Figure 5. Illustration of the inter- and intramolecular π -stacking interactions within the structure of $[\text{Ru}(\mathbf{4})](\text{PF}_6)_2$.

indicating a parallel displaced π - π stacking interaction, with the centroid of the catechol ring being 3.72 Å above bipy C5. This then extends to the next molecule with an intermolecular contact with the adjacent unit having the opposed helicity, with a separation of 3.59 Å above bipy C6' (Figure 3). Given the C_3 -symmetry, these interactions extend through the unit cell giving rise to the hexagonal packing in the lattice. The enclosed cavity comprised of the six oxygen atoms, with a *trans* distance from O1 to O3 across the unit being 4.998 Å, enclosing an empty void appropriate to take a small cation such as sodium or lithium, with the tertiary nitrogen also donating additional electron density into the cavity. Externally, the voids between the cations are filled with a combination of disordered water and acetonitrile, with the charge balance maintained by unidentified hydroxide units.

The structure of $[\text{Ru}(\mathbf{4})](\text{PF}_6)_2$ (Figure 4) was determined in the monoclinic system $P2_1/c$. In this case there is a lack of symmetry in the system with the Ru-N bond lengths and angles showing a wider discrepancy from the ideal, but still within an anticipated range (2.052 to 2.069 Å / 78.7 to 96.5° Table ESI 1). There is however a degree of disorder in two of the flexible ethylene linkages and one of the catechol rings, exhibiting a degree of planar rotation. In this case the cavity appears to be partially occupied (modelled at 0.67), not by a cation, but an oxygen atom, presumably in the form of water bonded by hydrogen bonds to both the phenyl ether oxygens and the ethylene CHs within the cavity (proton positions not determined). This suggests that either the nitrogen or oxygen is partially protonated with the O – H – N distance being 3.35 Å indicative of

a weak electrostatic interaction. Additionally, there is potential for at least one other hydrogen bond to the etheric oxygens with O – H – O separations in the range of 2.98 to 3.93 Å. This inclusion also results in a shortening of the long axis N to Ru separation to 7.915 Å in comparison to 8.780 Å found for $[\text{Ru}(\mathbf{4})](\text{OH})_2$ and regardless of the disorder, the plane of the catechol rings, whilst remaining in close contact to the adjacent pyridine rings, are now at a separation in the region of 3.70 to 3.98 Å above the bipyridine C4 position, rather than the C5 position, with a greater distortion from co-planarity (Figure 5). In addition, there is evidence of one intermolecular close contact between the catechol and the adjacent mirror image of the complex at 3.367 Å between the centroid of the ring and C4 of the bipyridine.

The electronic absorption spectra of $[\text{Ru}(\mathbf{4})]^{2+}$ in both acetonitrile, and aqueous solution are virtually identical to that of $[\text{Ru}(\text{bipy})_3]^{2+}$ with the characteristic metal-to-ligand charge transfer (MLCT) band occurring at 453 nm (Figure 6), although the π - π^* ligand centered transition at 290 is a notably broader absorption, with a greater extinction coefficient presumably arising from the additional phenyl-1,2-diol ether groups which absorb in a similar region to the bipyridine groups. Both the MLCT and π - π^* transitions in the spectrum were also invariant to the background ionic strength in the presence of a range of monovalent cations (Figure S4). The normalized emission spectrum of $[\text{Ru}(\mathbf{4})](\text{PF}_6)_2$ in aerated acetonitrile resulted in a maximum emission at 611 nm similar to that observed for $[\text{Ru}(\text{bipy})_3](\text{PF}_6)_2$, but with a slightly enhanced quantum yield of 0.058, assuming a quantum yield of 0.040 for $[\text{Ru}(\text{bipy})_3](\text{PF}_6)_2$

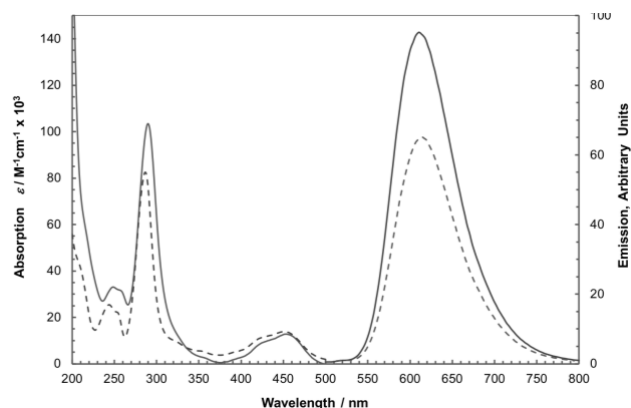


Figure 6. Absorption and emission spectra for [Ru(4)](PF₆)₂ (solid line) and [Ru(bipy)₃](PF₆)₂ (dashed) in CH₃CN at 298 K.

(Figure 6).^[29] The enhanced quantum yields are consistent with the observed pattern for caged complexes, and are of a similar order to those observed for structurally similar functionalized complexes.^[28b] The enhanced rigidity prevents ligand dissociation, whilst shielding the excited-state from quenching by O₂, due to inhibited access to one of the “pockets” along the C₃ axis of the cation.

The quantum yield of [Ru(4)]²⁺ relative to [Ru(bpy)₃]²⁺ in aerobic aqueous solution was a little lower than anticipated (Table 1). This suggests that the media changes the emissive properties significantly and can give rise to a significant component of the non-radiative (*k_{nr}*) decay process. Samples run in D₂O (97%) showed the anticipated isotropic effect when compared to samples run in H₂O, with an enhancement factor of 1.4, with a control sample of [Ru(bipy)₃]Cl₂ illustrating a similar enhancement (Figure S5).^[30] This indicates that in water there is a significant non-radiative deactivation due to the OH vibration mode of surrounding water molecules interacting with the excited-state located on the bipyridine groups through a charge transfer to solvent (CTTS) mechanism. For similar complexes, extended X-ray adsorption fine structural (EXAFS) analysis has shown that several water molecules are located along the C₃ axis of the complex within the second sphere^[31] strongly suggesting the existence of specific interactions with the ligand π -electrons. It is envisaged that a similar hydration sphere with water / D₂O being included within the cavity lying along the C₃ axis is occurring in this situation.^[32] In the presence of a large excess of small cations as chloride salts capable of occupying the cavity, such as Li⁺, Na⁺, K⁺, NH₄⁺, the emission was not significantly perturbed, remaining comparable to that of [Ru(4)₃](OH)₂ in aqueous solution (Table 1).

The addition of stoichiometric amounts of monovalent cations Li⁺, Na⁺, K⁺, NH₄⁺ as hexafluorophosphate salts to [Ru(4)₃](PF₆)₂ in acetonitrile resulted in no significant perturbation in the UV / vis absorption spectra (Figure S6). Similarly, the addition of up to ten equivalents of Li⁺, Na⁺, K⁺, NH₄⁺ as hexafluorophosphate salts, introduced to [Ru(4)](PF₆)₂ in both deuterated DMSO and acetone (Figure S7-10), resulted in no significant perturbation of the ¹H NMR spectrum, suggesting that there is marginal, if any, inclusion of these cations within the cavity. Given the observed inclusion of water in the solid-state, it is assumed that water (potentially as either H₃O⁺ or OH⁻) within the cavity is more strongly bonded than a competing monovalent cation.

Table 1. Electronic emission data for [Ru(4)]²⁺ at 298 K

Complex	Conditions	$\lambda_{\max} \pm 2$ nm	$\phi_{em} \pm 5\%$
[Ru(4)](PF ₆) ₂	CH ₃ CN	605	0.046
[Ru(bipy) ₃](PF ₆) ₂	CH ₃ CN	609	0.040 ^[29]
[Ru(bipy) ₃]Cl ₂	H ₂ O	610	0.028 ^[29]
[Ru(bipy) ₃]Cl ₂	D ₂ O	610	0.038
[Ru(4)] ²⁺	H ₂ O	611	0.020
[Ru(4)] ²⁺	D ₂ O	612	0.028
[Ru(4)] ²⁺	0.2 M HCl Aq	610	0.020
[Ru(4)] ²⁺	0.2 M LiCl Aq	610	0.019
[Ru(4)] ²⁺	0.2 M NaCl Aq	610	0.019
[Ru(4)] ²⁺	0.2 M KCl Aq	609	0.019
[Ru(4)] ²⁺	0.2 M NH ₄ Cl Aq	608	0.018

Given the tertiary amine in the structure, the variation in emissive behavior (relative quantum yield) with pH was investigated (Figure 7) by adjusting the pH sequentially with the addition of 0.2M aqueous sodium hydroxide solution, containing a standardized solution of [Ru(4)]²⁺ to a Britton–Robinson buffer solution, containing a standardized solution of [Ru(4)]²⁺ (abs. at 450 nm = 0.10). Between the region of pH 2 and pH 13, there is a gradual sigmoidal curve with a change in quantum yield of approximately 40%. Similar behavior has been seen in other amine functionalized systems,^[33] and this has also been observed in the deprotonation of appended phenolic units, and attributed to a photoinduced electron transfer (PET) process.^[34]

It is assumed that the ground-state *pK_a* of this system is equivalent to the excited-state *pK_a** given the remoteness of the protonation site relative to the chromophores. Further, the absorption spectra are effectively invariant with pH (Figure S11)

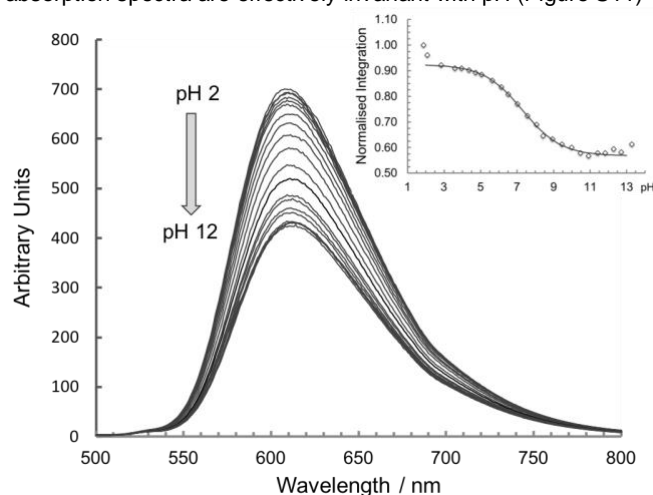


Figure 7 Variation in the emission spectra with pH for [Ru(4)]²⁺ introduced as [Ru(4)](OH)₂ in aqueous Britton–Robinson buffer solution and the sequential addition of 0.2M sodium hydroxide solution containing a standardized solution of [Ru(4)](OH)₂ (excited at 450 nm, absorption at 450 nm = 0.1 at 298 K). Inset the variation in normalized integration (proportional to quantum yield) for [Ru(4)]²⁺ with pH.

preventing the determination of the pK directly. The determination of the excited-state pK_a^* of $[\text{Ru}(\mathbf{4})]^{2+}$ proved to be non-trivial as application of the standard Henderson–Hasselbalch model failed to give a good fit, with the slope of the curve being far too shallow and extending across a remarkably large pH range (pH 3 to pH 12). A much better fit to the data was achieved using a standard Boltzman sigmoidal model, which includes a term to adjust for the shallowness of the curve, resulting in a pK_a^* of 7.26 ± 0.15 , which is consistent with the reported pK_a of triethanolamine (7.74).^[35]

The variation in excited-state lifetime of $[\text{Ru}(\mathbf{4})]^{2+}$ with pH range was also studied, again in a Britton–Robinson buffer solution and the sequential addition of aqueous sodium hydroxide. Consistent with the steady-state data, there was an almost linear decrease in the observed first order emissive lifetime τ_{em} from 0.50 μs to 0.42 μs as pH increases (Figure 8 and S12) commensurate with the opening up of an additional radiationless decay process. Under similar conditions, the long lived $^3\text{MLCT}$ emissive state of $[\text{Ru}(\text{bipy})_3]^{2+}$ is quenched via a variety of different non-radiative mechanisms including population of the ^3MC state, energy / electron transfer to oxygen, and through CTTS, at a collective rate of k_{nr} .^[17] The experimental emissive rate of decay k_{em} can be determined experimentally from the ratio of the quantum yield ϕ_{em} (0.020, Table 1) and the experimental emissive lifetime τ_{em} (Equation 1).

$$k_{em} = \phi_{em} / \tau_{em} \quad (1)$$

At pH 2, it can then be assumed that the experimental recorded emissive lifetime τ_{pH2} (0.505 μs) is a result of a combination of both the emissive and nonradiated rates (Equation 2), allowing for determination of the non-radiative rate constant k_{nr} (Equation 3).

$$1/\tau_{pH2} = k_{em} + k_{nr} \quad (2)$$

$$k_{nr} = (1 - \phi_{pH2}) / \tau_{pH2} \quad (3)$$

In the case of $[\text{Ru}(\mathbf{4})]^{2+}$, the act of deprotonation must open up an additional non-radiative decay route, the rate of which (k_{et}) can be determined at pH 12 from the shortened lifetime τ_{pH12} (0.417 μs) to be of the order of $k_{et} = 4.2 \times 10^5 \text{ s}^{-1}$ at 20 °C (Equations 4 and 5).

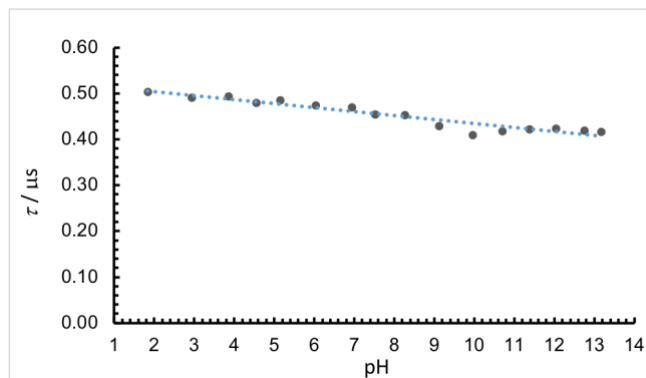


Figure 8 (a) Variation in emissive lifetime (τ) with pH of $[\text{Ru}(\mathbf{4})]^{2+}$ (introduced as $[\text{Ru}(\mathbf{4})](\text{OH})_2$) in aqueous Britton–Robinson buffer solution and the sequential addition of 0.2M sodium hydroxide solution at 298 K modelled as a single component exponential decay.

$$1/\tau_{pH12} = k_{em} + k_{nr} + k_{et} \quad (4)$$

$$k_{et} = 1/\tau_{pH12} - 1/\tau_{pH2} \quad (5)$$

The observed decay was also modelled as using two exponential functions, taking into account the increasing contribution from the electron transfer rate to the quenching as a function of pH. The values obtained are consistent with quenching observed in other related systems where the donor atom has a similar through space distance relationship, such as the electron transfer from phenothiazine (PTZ) to an excited state $[\text{Ru}(\text{bipy})_3]^{3+}$ unit.^[36] The complex $[\text{Ru}(\text{TAP})_2(\text{POQ-Nmet})]$ (where POQ-Nmet is 5-[4-[N-methyl-N-(7-chloroquinolin-4-yl)amino]-2-thiabutancarboxamido]-1,10-phenanthroline and TAP is 1,4,5,8-tetraazaphenanthrene) also shows similar pH behaviour with the rate affected by the buffer in solution.^[37] In the case of $[\text{Ru}(\mathbf{4})]^{2+}$, the rate is evidently tempered by the inclusion of the water located between the electron donor, and the acceptor.

At its simplest level, this quenching in emission can be attributed to the removal of a proton from the bridgehead nitrogen.

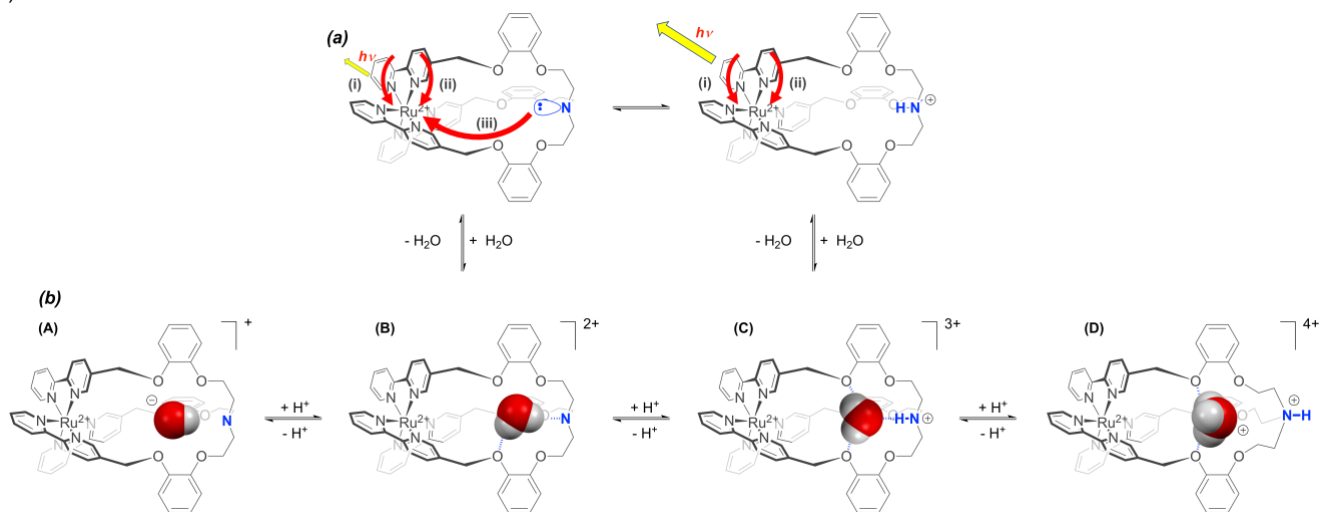


Figure 9 Schematic interpretation of the encapsulated water buffering the protonation of the tertiary amine in $[\text{Ru}(\mathbf{4})]^{2+}$ and an indication of the quenching processes (i) emissive, k_{em} , (ii) nonradiative, k_{nr} and (iii) electron transfer, k_{et} . (A) $(\text{OH}^-) : \text{NR}_3$; (B) $(\text{HO}^-) \cdots \text{H-N}^+\text{R}_3 \rightleftharpoons (\text{H}_2\text{O}) \cdots \text{NR}_3$ (C) $(\text{H}_2\text{O}) \cdots \text{H-N}^+\text{R}_3$ (D) $(\text{H}_3\text{O}^+) \cdots \text{H-N}^+\text{R}_3$

FULL PAPER

In the region of pH 3 to 4, it is reasonable to assume the tertiary nitrogen is effectively protonated whilst at high pH 10 to 13, the nitrogen is deprotonated, resulting in electron density capable of quenching the emission by a photoinduced electron transfer mechanism (PET) (Figure 9a). This is reinforced by the fact that the pK_a of triethanolamine is 7.74, in the middle of the observed range. But, given the exceptionally broad range over which the emissive quenching “grows” in, and that there is no fit to the standard Henderson–Hasselbalch equation, the inclusion of water in the cavity must play in an important role in the process. The included water can hydrogen bond to the bridgehead nitrogen, and to the ether oxygen atoms (as observed in the X-ray structure of $[\text{Ru}(\mathbf{4})](\text{PF}_6)_2$). The degree of protonation of the nitrogen is then dependent on the state of protonation of the included water molecule, so rather than having a single protonation, several states (A) to (C) could potentially be associated with the process (Figure 9b). It is also noted that at very low pH, the steady state emission shows an additional increase, which indicates a further protonation event that potentially then inverts the bridgehead nitrogen (situation D).

Conclusions

The synthesis of ruthenium complexes using podand type ligands remains a considerable challenge, and here we report a system in 35% yield, which whilst reasonable in comparison to related systems is still not satisfactory. We have demonstrated that it does impose a rigid and controlled facial geometry on the metal coordination, and in acetonitrile an enhanced emissive behavior, attributed to the increased rigidity reducing vibrational distortion and access to non-emissive metal centered orbitals. However, in aqueous solution the situation is far more complicated, where the enclosed cavity appears to allow inclusion of a water molecule. This facilitates a broad pH response via protonation of a remote tertiary amine, detectable by fluorescence spectroscopy. The encapsulated water is able to control the degree of PET quenching, effectively buffering the response through what is probably a three-stage process.

Experimental Section

Instrumentation: ^1H and ^{13}C NMR spectra were recorded on a Bruker Avance III 400 using the solvent as an internal reference, electronic absorption spectra were recorded on an Agilent Carey 60 UV vis spectrometer, fluorescence experiments were recorded in aerobic conditions on a Agilent Carey Eclipse spectrophotometer, quantum yields were determined by normalization against $[\text{Ru}(\text{bipy})_3]^{2+}$ in water (0.028) and acetonitrile (0.040).^[29] Lifetimes were determined in aerated aqueous solution, adjusting the pH with the sequential addition of 0.2M aqueous sodium hydroxide solution to a solution of $[\text{Ru}(\mathbf{4})]^{2+}$ in a Britton–Robinson buffer on a FluoTime 300 (PicoQuant) spectrometer equipped with a Peltier cooled photomultiplier (PMA-C, PicoQuant) with a 300 – 900 nm spectral range. All samples were photoexcited with a 480 nm picosecond pulsed laser at a 40MHz pulse repetition rate. Emission from the samples was detected at right angles to the excitation beam at 620 nm with a spectral bandwidth of 5 nm. The samples were excited using bursts of multiple pulses in order to improve sensitivity. All decay curves were fitted using single or two-exponential models using the FluoFit software (Picoquant). Microanalyses were performed by ASEP, the School of Chemistry, Queen's University Belfast.

Materials: 5-Methyl-2,2'-bipyridine,^[38] 5-bromomethyl-2,2'-bipyridine (1)^[25-26] and tris-2-chloroethylamine hydrochloride (3)^[27] were prepared by stated literature procedures. (Note extreme care must be exercised in the synthesis and handling of tris-2-chloroethylamine hydrochloride as it is a mustard agent with severe vesicant properties and isolated and used under license. All procedures using this material were undertaken in a fume hood using suitable gloves; all glassware was washed in an ethanolic base bath and remaining materials destroyed by reaction with KOH, and surfaces washed with bleach). Ethanol was dried by distillation under nitrogen from magnesium ethoxide. All other materials were purchased from Sigma Aldrich and used without purification.

2-[2,2']-Bipyridin-5-ylmethoxy-phenol (2): Catechol (16.17 g, 0.147 mol) was dissolved in dry ethanol (150 ml) and stirred under an N_2 atmosphere. K_2CO_3 (40.57 g; 0.294 mol) was added and the mixture refluxed for half an hour. A solution of 5-bromomethyl-2,2'-bipyridine (1) (6.00 g, 24.2 mmol) in dry ethanol (150 ml) was added and the resulting mixture was refluxed for 72 hrs. The reaction was cooled, and the solvent removed *in vacuo* to leave a dark residue which was dissolved in water (100 ml) and extracted with DCM (3 x 100 ml), and dried over MgSO_4 . The solvent removed and the residue dissolved in the minimum amount of EtOAc and precipitated by the addition of hexane. The solid was collected by filtration, then further recrystallized from hot toluene to give white powder. Yield, 1.70 g; 42%. ^1H NMR (300 MHz, CDCl_3) δ 5.18 (2H, s, CH_2), 5.80 (1H, s, OH), 6.85–6.97 (4H, m, ArH), 7.34 (1H, dd, $J = 5.2, 7.5$ Hz, bipyH^5), 7.86 (1H, d, $J = 8.4$ Hz, bipyH^4), 7.88 (1H, dd, $J = 7.5, 8.1$ Hz, bipyH^4), 8.41 (1H, d, $J = 8.1$ Hz, bipyH^3), 8.43 (1H, d, $J = 8.4$ Hz, bipyH^3), 8.69 (1H, d, $J = 5.2$ Hz, bipyH^6), 8.73 (1H, s, bipyH^6). ^{13}C NMR (75 MHz, CDCl_3) δ 68.9, (bipyCH_2), 112.7, 115.4, 120.6, 121.4, 121.6, 122.7, 124.3, 132.2 (q), 137.0, 137.4, 145.9 (q), 146.3 (q), 149.0, 149.6, 156.0 (q), 156.7 (q) (aromatic carbons). EI-MS: m/z 278 $[\text{M}]^+$ (12%), 169 $[\text{M}-\text{OC}_6\text{H}_4\text{OH}]^+$ (100%). IR (KBr disc) λ_{max} (cm^{-1}): 1274, 1214 (C–O stretch), 1463 (C–H bending), 1594, 1576, 1559, 1502 (ArC=C stretch), 3051 (Ar–H stretch), 3256 (OH stretch).

Tris-[2,2']-bipyridin-5-yl-methoxyphenoxyethyl)amine (4): Compound 2 (1.03 g; 3.69 mmol) was dissolved in dry ethanol (20 ml). NaH (60% in mineral oil, 0.16 g; 4.00 mmol) was added, upon which the orange solution became dark green and effervescence occurred. The solution was stirred until the effervescence ceased, then tris-(2-chloroethyl)amine hydrochloride (3) (0.22 g; 0.92 mmol) was added and the reaction heated at reflux for 38 hrs. The solvent was removed *in vacuo* and the solid residue dissolved in CHCl_3 (50 ml), washed with water (3 x 25 ml), and dried over MgSO_4 . The solvent was removed and the dark green residue triturated with methanol to give a beige solid, which was collected by filtration and dried in air. Yield, 0.67 g; 78%. Found: C: 70.14, H: 5.54, N: 9.79%; $\text{C}_{57}\text{H}_{51}\text{N}_7\text{O}_6 \cdot 2.5\text{H}_2\text{O}$ requires: C: 70.22; H: 5.79; N: 10.06%. ^1H NMR (300 MHz, CDCl_3) δ 3.24 (6H, t, $J = 5.7$ Hz, CH_2), 4.13 (6H, t, $J = 5.7$ Hz, CH_2), 5.09 (6H, s, bipyCH_2), 6.82–6.91 (12H, m, ArH), 7.27 (3H, dd, $J = 4.8, 7.5$ Hz, bipyH^5), 7.78 (3H, ddd, $J = 1.8, 7.5, 7.9$ Hz, bipyH^4), 7.82 (1H, dd, $J = 2.4, 7.9$ Hz, bipyH^4), 8.32 (6H, d, $J = 7.9$ Hz, $\text{bipyH}^{3,3}$), 8.67 (1H, dd, $J = 1.8, 4.8$ Hz, bipyH^6), 8.67 (1H, d, 2.4 Hz, bipyH^6). ^{13}C NMR (100 MHz, CDCl_3) δ 54.4, 68.0, 68.8 (alkyl carbons), 113.7, 115.1, 120.7, 121.0, 121.1, 122.2, 123.7, 132.9 (q), 136.2, 136.8, 148.1, 148.3 (q), 149.1, 149.3 (q), 155.6 (q), 155.8 (q) (aromatic carbons). ESMS: m/z 929 $[\text{M}]^+$ (17%), 469 $[\text{M}-\text{C}_{28}\text{H}_{20}\text{N}_4\text{O}_3]^+$ (66%).

$[\text{Ru}(\mathbf{4})](\text{PF}_6)_2$: Ligand 4 (0.10 g, 0.11 mmol) and AgNO_3 (0.10 g, 0.59 mmol) were dissolved in a mixture of ethanol (500 ml) and DMSO (50 ml) and heated to reflux. A solution of $\text{RuCl}_3 \cdot x\text{H}_2\text{O}$ (0.02 g, 0.11 mmol) in ethanol (100 ml) was added drop-wise using an addition funnel over 3 hrs and the resulting orange solution refluxed for a further 3 hrs. The ethanol was then removed *in vacuo* and NaCl (0.50 g, 1.4 mmol) was added to the red solution, which was then filtered and diluted with H_2O (350 ml) before being added to Sephadex® SP C-25 column ion exchange column. A bright orange band was eluted with 0.5 M aqueous NaCl solution and the product was precipitated by the addition of excess NH_4PF_6 . The resulting red solid was recrystallized from acetone/ water. Yield, 50 mg, 35%. Found: C: 48.97; H: 4.02; N: 6.75%, $\text{C}_{57}\text{H}_{51}\text{F}_{12}\text{N}_7\text{O}_6\text{P}_2\text{Ru} \cdot 4.5(\text{H}_2\text{O})$

requires C: 48.83; H: 4.31; N: 6.99 %. ^1H NMR (400 MHz, $(\text{CD}_3)_2\text{O}$) 2.91-2.99 (3H, m, NCH_2), 3.09-3.16 (3H, m, NCH_2), 3.97-4.04 (3H, m, NCH_2CH_2), 4.15-4.21 (3H, m, NCH_2CH_2), 5.20 (3H, d, $J = 14.5$ Hz, bipyCH_2), 5.43 (3H, d, $J = 14.5$ Hz, bipyCH_2), 6.62 (3H, d, $J = 8.0$ Hz, ArH), 6.85-6.91 (3H, m, ArH), 7.01-7.06 (6H, m, ArH), 7.59 (3H, ddd, $J = 1.2, 5.6, 7.8$ Hz, bipyH^5), 7.95 (3H, s, bipyH^6), 7.98 (3H, d, $J = 5.2$ Hz, bipyH^6), 8.08 (3H, dd, $J = 1.6, 8.0$ Hz, bipyH^4), 8.24 (3H, ddd, $J = 1.2, 7.8, 8.0$ Hz, bipyH^4), 8.61 (3H, d, $J = 8.0$ Hz, bipyH^3), 8.77 (3H, d, $J = 8.0$ Hz, bipyH^3). ESMS m/z 1176.2577(1) $[\text{M-PF}_6]^+$ (5 %), 515.6431(2) $[\text{M-2PF}_6]^{2+}$ (100 %). UV / vis λ_{max} , nm (ϵ , $\text{dm}^{-3} \text{mol}^{-1} \text{cm}^{-1}$) in CH_3CN at 298 K; 290 (882000), 453 (13900).

[Ru(4)(OH)]₂: $[\text{Ru}(4)](\text{PF}_6)_2$ (40 mg) was dissolved in acetonitrile (50 ml) and added to an aqueous suspension of old anion exchange resin Amberlite IRA-400 (chloride form) (100 ml) and stirred for 16 hrs. The resulting solution was filtered, and the volume of solvent reduced in vacuo to approx. 10 ml, and the product allowed to crystallize by slow evaporation.

X-ray crystallography: Crystals of $[\text{Ru}(4)](\text{PF}_6)_2$ were grown from 50% acetone / methanol by slow evaporation leading to small red blocks. Crystals of $[\text{Ru}(4)]\text{Cl}_2$ were harvested following slow evaporation from an aqueous solution. Single crystals were mounted on a Mitegen using Paratone-N oil and were cooled under a stream of nitrogen. Figures and tables were generated using OLEX2.^[39] Crystal data were collected on a Rigaku Oxford Diffraction SuperNova diffractometer using Cu K α radiation; the structures were solved by direct methods using ShelXT^[40] and refined by least squares using ShelXL.^[41]

Crystal Data CCDC No 1565969: for $\text{C}_{67}\text{H}_{51}\text{N}_{12}\text{O}_{13}\text{Ru}$ ($M = 1333.27$ g/mol): trigonal, space group R-3 (no. 148), $a = 15.8878(3)$ Å, $c = 47.1020(9)$ Å, $V = 10296.7(4)$ Å³, $Z = 6$, $T = 99.8(6)$ K, $\mu(\text{CuK}\alpha) = 2.423$ mm⁻¹, $D_{\text{calc}} = 1.290$ g/cm³, 56565 reflections measured ($5.628^\circ \leq 2\theta \leq 154.716^\circ$), 4850 unique ($R_{\text{int}} = 0.0367$, $R_{\text{sigma}} = 0.0139$) which were used in all calculations. The final R_1 was 0.0811 ($I > 2\sigma(I)$) and wR_2 was 0.2515 (all data).

CCDC No 1565970: for $\text{C}_{57}\text{H}_{51}\text{F}_{12}\text{N}_7\text{O}_7\text{P}_2\text{Ru}$ ($M = 1337.05$ g/mol): monoclinic, space group $P2_1/c$ (no. 14), $a = 22.2718(5)$ Å, $b = 12.46987(17)$ Å, $c = 22.0605(3)$ Å, $\beta = 107.783(2)^\circ$, $V = 5834.04(19)$ Å³, $Z = 4$, $T = 99.8(6)$ K, $\mu(\text{CuK}\alpha) = 3.547$ mm⁻¹, $D_{\text{calc}} = 1.522$ g/cm³, 30312 reflections measured ($8.174^\circ \leq 2\theta \leq 154.728^\circ$), 11804 unique ($R_{\text{int}} = 0.0458$, $R_{\text{sigma}} = 0.0568$) which were used in all calculations. The final R_1 was 0.0476 ($I > 2\sigma(I)$) and wR_2 was 0.1260 (all data).

Acknowledgements

We thank the School of Chemistry and Chemical Engineering (QUB) and The Chemistry Department (LU) for financial support. DELNI funded the studentship for RTB and we are grateful to the EPSRC mass spec. service in Swansea, and David Rochester (LU) for ESI data.

Keywords: Bipyridine • pH Sensor • Podand • Ruthenium • Tripodal ligands

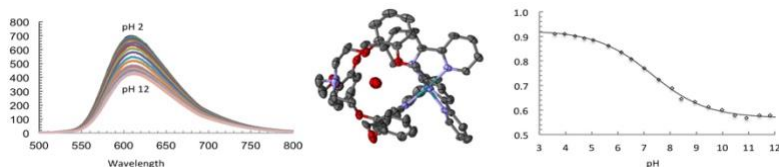
- [1] a) V. Amendola, M. Boiocchi, B. Colasson, L. Fabbrizzi, M. J. R. Douton and F. Uguzzoli, *Angew. Chem. Int. Edit.*, **2006**, *45*, 6920-6924; b) V. Amendola, M. Boiocchi, B. Colasson, L. Fabbrizzi, E. Monzani, M. J. Douton-Rodriguez and C. Spadini, *Inorg. Chem.*, **2008**, *47*, 4808-4816; c) V. Amendola, L. Fabbrizzi, C. Mangano, A. M. Lanfredi, P. Pallavicini, A. Perotti and F. Uguzzoli, *J. Chem. Soc., Dalton Trans.*, **2000**, 1155-1160; d) G. Frei, A. Zilian, A. Raselli, H. U. Güdel and H.-B. Burgi, *Inorg. Chem.*, **1992**, *31*, 4766-4773; e) S. Grammenudi and F. Vögtle, *Angew. Chem., Int. Ed. Eng.*, **1986**, *25*, 1122; f) J. C. Knight, S. Alvarez, A. J. Amoroso, P. G. Edwards and N. Singh, *Dalton Trans.*, **2010**, *39*, 3870-

- 3883; g) A. Lutz and T. R. Ward, *Helv. Chim. Acta*, **1998**, *81*, 207-218; h) A. Lutz, T. R. Ward and M. Albrecht, *Tetrahedron*, **1996**, *52*, 12197-12208; i) T. Nabeshima, S. Masubuchi, N. Taguchi, S. Akine, T. Saiki and S. Sato, *Tetrahedron Lett.*, **2007**, *48*, 1595-1598; j) T. Nabeshima, Y. Tanaka, T. Saiki, S. Akine, C. Ikeda and S. Sato, *Tetrahedron Lett.*, **2006**, *47*, 3541-3544; k) T. Nabeshima, Y. Yoshihira, T. Saiki, S. Akine and E. Horn, *J. Am. Chem. Soc.*, **2003**, *125*, 28-29; l) T. Nakamura, H. Kimura, T. Okuhara, M. Yamamura and T. Nabeshima, *J. Am. Chem. Soc.*, **2016**, *138*, 794-797; m) A. Pintér and G. Haberhauer, *Euro. J. Org. Chem.*, **2008**, 2375-2387; n) K. Sato, S. Arai and T. Yamagishi, *Tetrahedron Lett.*, **1999**, *40*, 5219-5222; o) P. Sheldon, W. Errington, P. Moore, S. C. Rawle and S. M. Smith, *Chem. Commun.*, **1994**, 2489; p) J.-E. S. Sonha and F. Fages, *Chem. Commun.*, **1997**, 327-329; q) G. Ulrich, S. Bedel and C. Picard, *Tetrahedron Lett.*, **2002**, *43*, 8835-8837; r) T. R. Ward, A. Lutz, S. P. Parel, J. Ensling, P. Gutlich, P. Buglyo and C. Orvig, *Inorg. Chem.*, **1999**, *38*, 5007-5017.
- [2] E. Zysman-Colman and C. Denis, *Coord. Chem. Rev.*, **2012**, *256*, 1742-1761.
- [3] L. Zelikovich, J. Libman and A. Shanzer, *Nature*, **1995**, *374*, 790-792.
- [4] a) R. Ballardini, V. Balzani, A. Credi, M. T. Gandolfi, F. Kotzbyba-Hilbert, J.-M. Lehn and L. Prodi, *J. Am. Chem. Soc.*, **1994**, *116*, 5741-5746; b) K. Sato, Y. Sadamitsu, S. Arai and T. Yamagishi, *Tetrahedron Lett.*, **2007**, *48*, 1493-1496.
- [5] L. Troian-Gautier and C. Moucheron, *Molecules*, **2014**, *19*, 5028-5087.
- [6] B. Pashaei, H. Shahroosvand, M. Graetzel and M. K. Nazeeruddin, *Chem. Rev.*, **2016**, *116*, 9485-9564.
- [7] P. T. Xu, N. S. McCool and T. E. Mallouk, *Nano Today*, **2017**, *14*, 42-58.
- [8] a) C. D. Windle and R. N. Perutz, *Coord. Chem. Rev.*, **2012**, *256*, 2562-2570; b) Y. Pellegrin and F. Odobel, *Coord. Chem. Rev.*, **2011**, *255*, 2578-2593; c) M. D. Doherty, D. C. Grills, J. T. Muckerman, D. E. Polyansky and E. Fujita, *Coord. Chem. Rev.*, **2010**, *254*, 2472-2482.
- [9] a) D. L. Ma, H. Z. He, K. H. Leung, D. S. H. Chan and C. H. Leung, *Angew. Chem.-Int. Edit.*, **2013**, *52*, 7666-7682; b) L. Salassa, *Eur. J. Inorg. Chem.*, **2011**, 4931-4947.
- [10] M. R. Gill and J. A. Thomas, *Chem. Soc. Rev.*, **2012**, *41*, 3179-3192.
- [11] M. H. Filby, J. Muldoon, S. Dabb, N. Fletcher, A. E. Ashcroft and A. J. Wilson, *Chem. Commun.*, **2011**, 559-561.
- [12] V. Fernandez-Moreira, F. L. Thorp-Greenwood and M. P. Coogan, *Chem. Commun.*, **2010**, *46*, 186-202.
- [13] F. Li, J. G. Collins and F. R. Keene, *Chem. Soc. Rev.*, **2015**, *44*, 2529-2542.
- [14] J. Van Houten and R. J. Watts, *Inorg. Chem.*, **1978**, *17*, 3381-3385.
- [15] B. Durham, J. V. Caspar, J. K. Nagle and T. J. Meyer, *J. Am. Chem. Soc.*, **1982**, *104*, 4803-4810.
- [16] a) L. de Cola, F. Barigelletti, V. Balzani, P. Belsler, A. Von Zelewsky, F. Vogtle, F. Ebmeyer and S. Grammenudi, *J. Am. Chem. Soc.*, **1988**, *110*, 7210-7212; b) R. F. Beeston, S. L. Larson and M. C. Fitzgerald, *Inorg. Chem.*, **1989**, *28*, 4187-4189.
- [17] a) F. Barigelletti, L. De Cola, V. Balzani, P. Belsler, A. von Zelewsky, F. Vögtle, F. Ebmeyer and S. Grammenudi, *J. Am. Chem. Soc.*, **1989**, *111*, 4662-4668; b) R. F. Beeston, W. S. Aldridge, J. A. Treadway, M. C. Fitzgerald, B. A. DeGraff and S. E. Stitzel, *Inorg. Chem.*, **1998**, *37*, 4368-4379; c) H. Dürr, R. Schwarz, C. Andreis and I. Willner, *J. Am. Chem. Soc.*, **1993**, *115*, 12362-12365.
- [18] S. L. Dabb and N. C. Fletcher, *Dalton Trans.*, **2015**, *44*, 4406 - 4422.
- [19] K. D. Oylar, F. J. Coughlin and S. Bernhard, *J. Am. Chem. Soc.*, **2007**, *129*, 210-217.
- [20] H. Weizman, J. Libman and A. Shanzer, *J. Am. Chem. Soc.*, **1998**, *120*, 2188-2189.
- [21] a) N. C. A. Baker, N. C. Fletcher, P. N. Horton and M. B. Hursthouse, *Dalton Trans.*, **2012**, *41*, 7005-7012; b) N. C. Fletcher, R. T. Brown and A. P. Doherty, *Inorg. Chem.*, **2006**, *45*, 6132-6134; c) N. C. Fletcher, C. Martin and H. J. Abraham, *New J. Chem.*, **2007**, *31*, 1407-1411.
- [22] N. C. Fletcher, R. Prabaharan, M. Nieuwenhuyzen and A. Wilson, *Chem. Commun.*, **2002**, 1188-1189.
- [23] C. Hamann, A. von Zelewsky, A. Neels and H. Stoeckli-Evans, *Dalton Trans.*, **2004**, 402-406.
- [24] P. Alreja and N. Kaur, *RSC Adv.*, **2016**, *6*, 23169-23217.
- [25] J. Eaves, H. Munro and D. Parker, *Inorg. Chem.*, **1987**, *26*, 644-650.

- [26] S. A. Savage, A. P. Smith and C. L. Fraser, *J. Org. Chem.*, **1998**, *63*, 10048-10051.
- [27] a) J. M. Baumeister, R. Alberto, K. Ortner, B. Spingler, P. A. Schubiger and T. A. Kaden, *J. Chem. Soc. Dalton Trans.*, **2002**, 4143-4151; b) K. Ward, *J. Am. Chem. Soc.*, **1935**, *57*, 914-916.
- [28] a) N. C. Fletcher, M. Nieuwenhuyzen and S. Rainey, *J. Chem. Soc., Dalton Trans.*, **2001**, 2641-2648; b) R. T. Brown, N. C. Fletcher, M. Nieuwenhuyzen and T. E. Keyes, *Inorg. Chim. Acta.*, **2005**, *358*, 1079-1088.
- [29] K. Suzuki, A. Kobayashi, S. Kaneko, K. Takehira, T. Yoshihara, H. Ishida, Y. Shiina, S. Oishic and S. Tobita, *Phys. Chem. Chem. Phys.*, **2009**, *11*, 9850-9860.
- [30] a) W. R. Cherry and L. J. Henderson, **1984**, *23*, 983-986; b) J. van Houten and R. J. Watts, *J. Am. Chem. Soc.*, **1975**, *97*, 3843-3844.
- [31] H. Yokoyama, K. Shinozaki, S. Hattori and F. Miyazaki, *Bull. Chem. Soc. Jpn.*, **1997**, *70*, 2357-2367.
- [32] A. A. Abdel-Shafi, M. D. Ward and R. Schmidt, *Dalton Trans.*, **2007**, 2517-2527.
- [33] P. D. Beer and J. Cadman, *New J. Chem.*, **1999**, *23*, 347-349.
- [34] a) R. Grigg, J. M. Holmes, S. K. Jones and W. D. J. A. Norbert, *J. Chem. Soc., Chem. Commun.*, **1994**, 185-187; b) A. M. W. Cargill-Thompson, M. C. C. Smailes, J. C. Jeffery and M. D. Ward, *J. Chem. Soc., Dalton Trans.*, **1997**, 737-743.
- [35] M. R. Simond, K. Ballerat-Busserolles, Y. Coulier, L. Rodier and J. Y. Coxam, *J. Sol. Chem.*, **2012**, *41*, 130-142.
- [36] S. L. Larson, C. M. Elliott and D. F. Kelley, *Inorg. Chem.*, **1996**, *35*, 2070-2076.
- [37] A. Del Guerso, A. Kirsch-de-Mesmaeker, M. Demeunynck and J. Lhomme, *J. Phys. Chem. B*, **1997**, *101*, 7012-7021.
- [38] T. L. J. Huang and D. G. Brewer, *Can. J. Chem.*, **1981**, *59*, 1689-1700.
- [39] O. V. Dolomanov, L. J. Bourhis, R. J. Gildea, J. A. K. Howard and H. Puschmann, *J. Appl. Crystallogr.*, **2009**, *42*, 339-341.
- [40] G. M. Sheldrick, *Acta Crystallogr. Sect. A*, **2015**, *71*, 3-8.
- [41] G. M. Sheldrick, *Acta Crystallogr. Sect. A*, **2008**, *64*, 112-122.

Entry for the Table of Contents (Please choose one layout)

FULL PAPER



A Ru²⁺ trisdiimine complex with C₃-symmetry and a cryptand like cavity is reported. This shows enhanced emission compared to [Ru(bipy)₃]²⁺ in CH₃CN, but is significantly quenched in water. This is invariant to the presence of salt, but decreases further with increasing pH attributed to a switchable electron transfer mechanism controlled by the degree of protonation of an included water molecule.

Key Topic* Ru, Cavitand, pH

Rodney T. Brown,^[b] Nicholas C. Fletcher,^{*,[a,b]} Lefteris Danos^[a] and Nathan R. Halcovitch^[a]

Page No. – Page No.

A Tripodal Ruthenium(II) Polypyridyl Complex with pH controlled Emissive Quenching